

2017

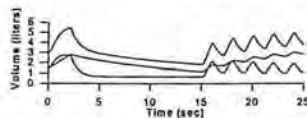
CHARACTERISTICS OF AEROSOLS GENERATED DURING A COUGH. D.G. Frazer, W.T. Goldsmith, A.A. Afshari, N. Phillips, K.C. Weber and E.L. Peterson, PPRB, HELD and CIB DRDS, NIOSH, MORGANTOWN, W.V. 26505.

A system including a spirometer and LAS-X particle analyzer was designed to examine aerosols generated during a cough. The system was held at 37°C in a temperature controlled chamber. Air was pulled through a HEPA filter and the spirometer at a constant rate (5 l/min) so that aerosols introduced to the spirometer-aerosol analyzer system were continuously washed out. A subject breathing ambient air coughed into the spirometer, then breathed HEPA filtered air and coughed at 2 min intervals for 6 min. Background aerosol measurements were recorded prior to each cough. Preliminary experiments showed that the difference in the number of particles recovered from the spirometer with respect to background (NPD) was greatest following the first cough, was reduced during the second cough, but tended to increase following the third and fourth coughs. Particle diameters ranged between 0.1 and 5.0 µm after each cough, and more than 95% of the particles had diameters less than 1.0 µm. Results also showed that there was a significant variation in NPD (±300%) between subjects following each of the four coughs.

2019

Computer Simulation of Ventilation After Lung Volume Reduction Surgery (LVRS) or Lung Transplantation (LT). S.H. Loring and D.E. Leith, Beth Israel Deaconess Medical Center, Boston, MA 02215.

LVRS and LT change the mechanical relationships among left and right lungs and chest wall for good or ill. We developed a computer model that simulates pre-operative and predicts post-operative ventilatory function using a patient's preoperative mechanical characteristics and assumed normal properties for transplanted lung or reduced lung compliance due to reduced lung mass after LVRS. Pressure-volume characteristics of each lung are represented by the coefficients of Salazar and Knowles, and pressure-flow characteristics are fitted to spirometric data. Expiratory flow limitation is simulated for each lung according to the equal pressure point formulation of Mead. The mediastinum is assumed to be compliant, and chest wall pressures are simulated during selected patterns of ventilatory muscle activity and relaxation. The Figure shows individual and summed volume-time plots of a native emphysematous lung and a normal transplanted lung during a forced vital capacity and forced hyperpnea. During hyperpnea, the native lung becomes progressively hyperinflated while the transplanted lung becomes progressively less inflated as average pleural pressures become more positive. (Supported by HL-52586.)



2018

CUMULATIVE GAS TRAPPING IN ASSOCIATION WITH INFLATION/DEFLATION CYCLES IN EXCISED RAT LUNGS. G. N. Franz and D. G. Frazer, West Virginia Univ. School of Medicine, HSC-N, Box 9229, Morgantown, WV 26506-9229, and Division of Respiratory Disease Studies, NIOSH, Morgantown, WV 26505.

In the first case considered, inflation of excised rat lungs to 50% of TLC and subsequent deflation to an end-expiratory pressure of -5cm H₂O produces a new, higher residual volume due to the "trapping" of gas by previously inflated lung units. Re-inflating the lung to the previous end-expiratory volume plus the volume of the previously trapped gas produces a deflation curve very similar to the preceding one, except for a parallel upward shift. Successive re-inflations and deflations produce a family of volume-pressure curves with these characteristics: (1) the volume change upon inflation stays fixed as the end-inspiratory volume is always incremented by the gas volume trapped in the previous cycle, (2) re-inflation starts from ever higher end-expiratory volumes as the trapped gas volume cumulatively rises, and (3) deflation curves of nearly identical shape are shifted upward in a parallel manner as they start from an ever higher end-inspiratory volume.

In the second case considered, the lungs are inflated to TLC and then deflated to an end-expiratory pressure of -5cm H₂O. Successive re-inflation/deflation cycles generate cumulative additions to trapped gas volume. While the end-inspiratory volume stays at about TLC, end-expiratory volume rises as progressively smaller increments of trapped gas volume are revealed by successive deflations. The preceding phenomena are compatible with these notions: (1) gas trapping occurs during inflation, (2) the gas volume trapped in a lung unit is close to that unit's maximal volume, (3) peripheral units experience trapping before central units, and (4) gas trapping in some units makes it easier for other units to undergo gas trapping on a subsequent re-inflation.

2020

DIAPHRAGM SHORTENING DURING PRESSURE SUPPORT VENTILATION.

J. Pierce, J. Trank, E. Gilliland, N. Smith-Blair and R. Clancy, University of Kansas Medical Center, Kansas City, KS 66160.

The aim of this study was to determine the effect of pressure support ventilation (PSV) on diaphragm shortening (DS) and other cardiopulmonary parameters. DS was measured using a single crystal ultrasonic transducer glued to the inferior surface of the right hemidiaphragm. DS is expressed as the change in diaphragm thickness during inspiration divided by diaphragm thickness at end expiration. This ratio is defined as fractional thickening (FT). In 15 anesthetized Sprague-Dawley male rats, PSV was increased from 0 to 10 cm H₂O in 2 cm H₂O increments every 2 mins. At each level of PSV the following parameters were measured: respiratory rate (RR), end-tidal CO₂ (EtCO₂), tidal volume (V_t), positive inspiratory pressure (PIP), intrathoracic pressure (ITP) and FT. Increasing PSV to 10 cm H₂O resulted in: RR ↓ by 25% and EtCO₂ ↓ by 9%. Whereas, increasing PSV to 10 cm H₂O resulted in: V_t ↑ by 5 cc, PIP ↑ by 9.4 cm H₂O, CVP ↑ by 98%, and ITP ↑ by 55%. All of the above changes were statistically significant at p < 0.05. Increasing PSV from 0 to 10 cm H₂O resulted in FT ↑ by 10%, however this was not statistically significant. In conclusion, the decrease in the work of breathing due to PSV was not associated with a decrease in diaphragm shortening as measured by FT. (NIH NINR KO7NR00059-03)

CONTROL OF BREATHING II (2021-2022)

2021

RESPIRATORY EFFECTS OF A PRENATAL DIETARY PROTEIN RESTRICTION ON MATURE RATS. P. Gressens, S. M. Muaku, L. Besse, E. Nsegebe, J. Gallego, B. Delpech, C. Gaultier, P. Evrard, J. M. Ketelslegers and D. Maitre.

Robert-Debré Hospital, Paris, Henri-Becquerel Center, Rouen, France, University of Louvain Medical School, Brussels, Belgium.

We studied the hypoxic response of ten rats exposed to a prenatal dietary protein restriction during the two first weeks of gestation. Breathing pattern was measured using a whole body plethysmograph. Each animal received 3 hypoxic tests consisting of a linear decrease in F_iO₂ from 21% to 8% in 3 min. Hypoxic responses were grossly similar in depleted and control rats. However, V_T and V_I increased during the 30 first seconds of hypoxia in the depleted rats, whereas V_T and V_I decreased in controls (interaction P<0.017). These changes were due to changes in V_T, not T_{70%}. In the depleted rats, the time to peak V_T significantly decreased from 199±32 sec in the first test to 156±27 s in the third test, whereas it did not vary in controls (interaction P<0.016). Taken together, these data suggested that the hypoxic depression was slightly impaired in mature rats which have been exposed to protein restriction during gestation.

Supported by CRI INSERM

2022

HYPOXIA DOES NOT ALTER BREATHING PATTERN IN FLYING MAGPIES (*Pica pica*). D.F. Boggs, R.W. Bavis, D.L. Kilgore, Jr., P.M. Schmitt and K.P. Dial, The University of Montana, Missoula, MT 59812.

Magpies and other birds tend to coordinate respiratory and wingbeat cycles to minimize the mechanical interference and to maximize the potential assistance of the wingbeat cycle to ventilation. We previously demonstrated that stimulating breathing with 5% CO₂ in flight did not disrupt this coordination. Because hypoxia is more likely than hypercapnia to alter respiratory frequency, we exposed 3 magpies to 12% O₂ (P_iO₂ = 82 torr, equivalent to an altitude of 5,200m) while flying in a wind tunnel at their preferred speed (6-7 m s⁻¹). We found that although this level of hypoxia significantly increased respiratory frequency in the resting birds (from 41.3 ± 1.4 (S.D.) to 55 ± 0.8 breaths min⁻¹) it had no effect on respiratory frequency in flying birds (164.2 ± 13.8 normoxia vs 166.8 ± 18.5 hypoxia), and since the wingbeat frequency was also unchanged the ratio of flaps to breaths remained the same. Interclavicular airsac gas measurements indicate that there is a hyperventilation in flight:

	Rest		Flight	
	PO ₂ (torr)	PCO ₂ (torr)	PO ₂ (torr)	PCO ₂ (torr)
normoxia (n=3)	89.6 (±2.1)	33.9 (±3.1)	101.6 (±0.25)	27.3 (±1.65)
hypoxia (n=2)	44.7	27.3	58.5	20.8

Hyperventilation with flight may have raised PO₂ sufficiently to remove this moderate hypoxic stimulus to increase frequency, or the control mechanisms responsible for respiratory-locomotor cycle coordination may be more influential than chemoreceptor input in controlling breathing pattern.

THE FASEB JOURNAL

Volume 11, Number 3

February 28, 1997

ABSTRACTS

SUNDAY MORNING

April 6, 1997

Physiology

- Refresher Course for Teaching Respiratory
Physiology A1

Anatomy

- Cytoskeleton and Adhesion in Endothelial Cells A1
Signal Transduction and Cell Migration A3

SUNDAY AFTERNOON

April 6, 1997

Physiology

- Neural Control of Circulation I A4
Neural Regulation of the Kidney A6
Renal Transport: Ions and Receptors A8
Nitric Oxide I A10
Muscle Fatigue A12

Nutrition

- Zinc Metabolism I A14

Anatomy

- Cardiovascular Development A16

MONDAY MORNING

April 7, 1997

Physiology

- Carl Ludwig Distinguished Lectureship
Minisymposium A17
Cellular and Tissue Engineering A18
Cerebral Circulation A20
Renal Transport: Water and Urea A22
Ionic Homeostasis and Volume Regulation A24
Endothelial Factors and Renal Function A26
Scholander Award Session A27
History of Physiology A31
Transporters A31
Cell Biology of White Cells and Platelets A32

- Gastrointestinal Motility A33
Mucosal Absorption and Transport A34
Pulmonary Hypertension A35
Hypertension I A37
Microcirculation A40
Neural Control of the Heart A45
Neural Control of Circulation II A47
Exercise Responses I A51
Skeletal Muscle Physiology A54
Smooth Muscle Physiology and Pharmacology A59
Contractile and Regulatory Proteins A61
Growth Factors and Receptors: Vascular Biology
and Angiogenesis A62
Cardiac Myocytes A64
Free Radical Injury (Cardiac and Vascular) A68
Myocardial Ischemia I A70
Endothelium A75
Endothelial Factors and Cardiovascular-Renal
Homeostasis A77
Endothelium-Dependent Responses I A78
Renal Pathophysiology/Metabolism A82
Renin-Angiotensin/Renal Microvascular
Regulation A84
Temperature Response I A87
Comparative Physiology A90
Gravitational A96
Endocrine Pharmacology A99

Pathology

- Molecular Markers of Cancer A100
Leukocyte-Endothelial Cell Interactions A101
Hepatic Progenitor Cells and Regeneration A103
Acute Lung Injury A105
Neuropathobiology A106
Ca²⁺ Signaling A109
Arachidonic Acid Metabolism A111
Inflammatory Response I A113
Inflammatory Mediators and Cell Injury A119
Oxidant Injury/Hyperoxia A121
Pulmonary Cell Injury, Inflammation and
Gene Expression A123
Acute Lung Injury A126
Control of Breathing I A130
Pulmonary Vascular Biology I A134
Vascular Pathobiology A137

Nutrition

- Lipid and Fatty Acid Metabolism and Transport A138